Journal of Applied Polymer Science

Synergistic reinforcement of NBR by hybrid filler system including organoclay and nano-$CaCO_3$

Sina Salkhord,[1] Hedayatollah Sadeghi Ghari[2]
[1]Department of Polymer Engineering, Islamic Azad University, Mahshahr Branch, Mahshahr, Iran
[2]Young Researchers and Elite Club, Islamic Azad University, Omidieh Branch, Omidieh, Iran
Correspondence to: S. Salkhord (E-mail: sina.salkhord@gmail.com)

ABSTRACT: Rubber nanocomposites containing one type of nanofiller are common and are widely established in the research field. In this study, nitrile rubber (NBR) based ternary nanocomposites containing modified silicate (Cloisite 30B) and also nano-calcium carbonate (nano-$CaCO_3$) were prepared using a laboratory internal mixer (simple melt mixing). Effects of the hybrid filler system (filler phase have two kind of fillers) on the cure rheometry, morphology, swelling, and mechanical and dynamic–mechanical properties of the NBR were investigated. Concentration of nano-$CaCO_3$ [0, 5, 10, and 15 parts per one hundred parts of rubber by weight (phr)] and organoclay (0, 3, and 6 phr) in NBR was varied. The microstructure and homogeneity of the compounds were confirmed by studying the dispersion of nanoparticles in NBR via X-ray diffraction and field emission scanning electron microscopy. Based on the results of morphology and mechanical properties, the dual-filler phase nanocomposites (hybrid nanocomposite) have higher performance in comparison with single-filler phase nanocomposites. © 2015 Wiley Periodicals, Inc. J. Appl. Polym. Sci. **2015**, *132*, 42744.

KEYWORDS: mechanical properties; nanostructured polymers; rubber

Received 6 November 2014; accepted 14 July 2015
DOI: 10.1002/app.42744

INTRODUCTION

One of the most important phenomena in material science is the reinforcement of rubber by rigid entities, such as carbon black (CB), clays, silicates, and calcium carbonate. Thus, these fillers, or reinforcement aids, are added to rubber formulations to optimize the properties that meet a given service application or sets of performance parameters.[1] Clay is hydrous aluminum silicate consisting of platelets that has high aspect ratio; therefore, it has a considerable influence on the mechanical properties and permeability. Organoclay is a kind of commonly used nanoscale filler for polymers due to its excellent mechanical properties, barrier property, and thermal stability. Layered silicates existing on a nanoscale are effective reinforcements for rubber materials.[2–5] However, the complete and homogeneous dispersion of individual silicate layers in a rubber matrix is difficult to realize, and there are still no generally applicable guidelines for the optimum rubber/layered-silicate combination, especially by means of a conventional rubber-compounding process.[6]

Reinforcing fillers are fundamental ingredients in the manufacture of rubber products, due to their unique ability to enhance the physical properties of elastomers. A number of mineral fillers (calcium carbonate, clays, silica, silicates, and talc) are used in the rubber industry to extend and/or reinforcing of elastomers. CB is always considered as the most consuming reinforcing filler in rubber industry. Considering its problems like its darkness and contamination, researchers are seeking an adequate alternative for it. Calcium carbonate is one of the most abundant white minerals in the earth's sedimentary crust. It is probably one of the most widely used mineral additives because of its whiteness, low abrasion, availability in wide-size ranges, and low cost. Organoclay may become suitable substitute as filler in applications where CB and silica are currently dominant or combine with them to produce hybrid reinforcement for rubber compounds. Most of the published research papers on rubber nanocomposites investigate the use of nanoclay as the only active filler in the rubber compound. Trying to improve the rubbers properties using nanoclay are still continuous. Recently, researchers have investigated the combination of nanostructured silica or CB and nanoclay fillers.[7–9] One very important output of these investigations was the synergy experienced between layered nanoclays and silica or CB. The incorporation of industrial and agricultural waste such as olive solid by-product, marble waste, rice husk, and agro polymer based olive solid as hybrid fillers in rubber nanocomposite were reported.[10–12] The incorporation of agro polymer-based olive solid waste into the carboxylated nitrile rubber (XNBR)–organoclay (Nanofil 15) nanocomposites had improved the mechanical properties compared to XNBR/organoclay as well as XNBR

gum vulcanizate.[13] Relative efficiency of different types of fillers (phenolic resin, CB and CB plus phenolic resin) hybrid system in nitrile rubber (NBR) vulcanizates for the improvement of physico-mechanical properties, resistance to swelling in oil/fuel and thermal stability has been studied.[14] The hybrid filler system was always found to offer maximum benefit in strength and dynamic mechanical properties coupled with higher percent of retention of physical properties due to aging and swelling resistance in oil or fuel. The laboratory electrolytic cleaning tank immersion test results showed that hybrid filler system ((natural rubber)/clay + CB) had the best hardness and resistivity stability after the immersion test and so higher environmental resistance properties for NR.[15] The effects of partial replacement of palm ash by silica on curing characteristics, mechanical properties, and morphology of NR hybrid palm ash/silica composites were also investigated.[16] The increment of silica loading in the weight ratio of silica/palm ash enhances the rubber–filler interaction, tensile properties, shorter curing time, and fatigue life of NR hybrid composites. It has been shown that the NR,[17,18] styrene butadiene rubber (SBR)[19], and NBR[20] vulcanizates containing silica/CB give better overall mechanical properties and good balance in the properties compared to those having only 50 phr of silica or CB. The explanation is given as the better filler dispersion as a result of the lower development of filler network in the vulcanizates.

Combination of CB + carbon nanotube,[21–28] organoclay + nanosilica,[29,30] organoclay + carbon nanotube,[31] CB + Graphene,[32] organoclay + nano-$CaCO_3$,[33] and short jute fibers + carbon nanotube[34] was also the subject of some studies in rubber–hybrid filler nanocomposites. The synchronous use of CB and nanoclay has been reported. Herrmann[35] reported the considerable improvement of mechanical properties for hydrogenated NBR system containing CB and organoclay in comparison with the system reinforced with a type of filler. The synergistic effect between CB and organoclay, such as in mechanical and dynamic mechanical properties in rubbers (NR,[36–39] epoxidized natural rubber (ENR),[40,41] SBR,[42–45] poly(1,4-cis-isoprene),[46] ethylene–propylene–diene rubber (EPDM),[47] chlorobutyl,[48] polyurethane and bromobutyl[49] and etc) was also investigated. For example, for the CB/organoclay hybrid nanocomposites, the enhanced mechanical and thermal properties were observed at 2 phr of organoclay and 8 phr of CB. This has been attributed to the synergistic effect of both fillers. Synergistic effect of CB in presence of nanofillers (nanoclay and nanofiber) on mechanical and dynamic mechanical properties of NR/nanoclay/CB and NR/carbon nanofiber (CNF)/CB nanocomposites was discussed in light of electrostatic interactions and the concomitant microstructural developments.[50] It was observed that the mechanical and dynamic mechanical properties of these nanocomposites were much better compared with those of either NR/nanoclay or NR/CNF nanocomposites or the NR/CB microcomposite. These nanocomposites exhibited 18% increment in tear strength, 40% in modulus at 300% elongation, and 326% in room temperature storage modulus over the microcomposite. TEM micrographs of the nanocomposites showed that CB formed "nano-blocks" of reinforcement—close association of nanofiller and black—driven by zeta potential differences between the black and the nanofillers. The synergistic mechanism was generally explained that the coexistence of organoclay and CB could enhance the organoclay–CB network structure, which can hinder the movement of polymer chains and thus improve the mechanical properties.[7,37,51]

Liu *et al.*[52] showed that hybrid filler (organoclay and CB) was promising in the enhancement of long-term durability in engineering rubber applications by delaying the catastrophic crack propagation. Hybrid CB (N330 and N754) and organoclay (Cloisite 15A and 20A) in NR nanocomposites with emphasis on the fatigue and cut resistance have provided superior mechanical performances over conventional composites. The fatigue crack growth test showed that the hybrid-filled specimens exhibited better crack resistance black-filled samples at higher tearing energy region. Bhattacharya reported synergy in tribological characteristics of NR hybrid (organoclay + CB) nanocomposites.[53] Wear loss was reduced in the hybrid nanocomposites by 33% (over the CB microcomposite) in less stringent and 75% under severe wear conditions. These hybrid-filled nanocomposites also illustrated good wet skid, low rolling resistance, and lowering of coefficient of friction and heat build-up due to the formation of a unique microstructural architecture by the participating fillers.

Achieving a method in which the nanoparticles fillers can be dispersed adequately in polymer matrix is always a challenge in polymer nanocomposites. This research is aimed at presenting a new procedure to achieve higher mechanical performance of hybrid filler system (organoclay and nano-$CaCO_3$) in rubber nanocomposites. Combination of organoclay and nano-$CaCO_3$ was also the subject of our study and our effort to identify the most cost-effective rubber compounds which optimize mechanical properties. In this article, melt intercalation method were used for the preparation of NBR/organoclay/nano-calcium carbonate nanocomposites. Yet, now there is not any report about reinforcing the NBR using two fillers namely nano-$CaCO_3$ and organoclay. In this paper, reinforcing capability of nano-$CaCO_3$ (nanoparticle) and organoclay (nanolayer) in NBR on the morphology, cure rheometry, mechanical behaviors, and swelling resistance of NBR has been evaluated.

EXPERIMENTAL

Materials

The commercially available NBR used in this study was KNB-35L with Mooney viscosity ML [1 + 4,100] = 50 from south Korea. Organically modified montmorillonite (organoclay) was purchased from Southern Clay Products (Gonzales, TX) under the trade name of Cloisite 30B. This organoclay was modified by methyl tallow bis-2-hydroxyethyl quaternary ammonium with a concentration of 90 meq/100 g of clay (see Fig. 1). Nano-Calcium carbonate (Socal-312) was supplied by the Solvay Chemicals International Company from Belgium. Socal 312 is an ultrafine surface-treated precipitated calcium carbonate. The applied particle sizes were 50–90 nm. The ingredients (zinc oxide, stearic acid, and sulfur) were purchased from local suppliers (analytical grade). N-t-butyl-2-benzothiazole sulfonamide (TBBS) was supplied by the Reliance Technochem from Thailand, IPPD 4010NA antioxidant from Bayer Company

Table I. Nanofiller Compositions Parts per Hundred Parts of Rubber (phr) and Abbreviations of the NBR Nanocomposites

Compounds	Organoclay	$CaCO_3$
Pure NBR	-	-
NC300	3	-
NC305	3	5
NC310	3	10
NC600	6	-
NC605	6	5
NC610	6	10

(Germany), and toluene for swelling experiment was supplied by Merck.

Preparation of Hybrid NBR Nanocomposites

All the rubber nanocomposites were prepared with the rate of 60 rpm at 70°C in a laboratorial internal mixer (Brabender from Germany with volume 300 cc). The compositions of the used nanofillers for preparation of nanocomposites are listed in Table I. For mixing, the ingredients of nanocomposites, firstly NBR, were masticated and then organoclay and nano-calcium carbonate simultaneously were added to NBR and mixed. In a previous study,[54] order of mixing of the nano-fillers into internal mixer was studied and the obtained results showed that the synchronous addition of two nano-fillers to NR leads to achieving the most efficient performance. Then zinc oxide, stearic acid, and antioxidant were added to the compound. The content of zinc oxide, stearic acid, antioxidant, TBBS, and sulfur used in all compounds is 5 phr, 2 phr, 1 phr, 1 phr, and 2 phr, respectively. NBR/CB-30 sample was prepared by same formulation, but used 30 phr N330 CB. After mixing, the rubber compounds were left for 12 h and then sulfur and accelerator were added.

To prepare specimens for measuring the physical and mechanical properties, the compounds were cured into 2 mm thick sheets in a standard mold at 150°C under pressure of 10 MPa in an electrically heated hydraulic press according to their respective cure times (T_{95}), which were determined by using an oscillating disk rheometer Figure 1.

Characterization

Cure Characteristics. Curing characteristics of nanocomposites were measured according to ASTM D2084-95 by using Oscillating Disc Rheometer (Monsanto Rheometer 100 from USA) operated at 150°C with 1° arc oscillation angle. Scorch time (T_S), optimum cure time (T_{95}), and also the minimum torque (M_L), maximum torque (M_H), and the difference between minimum and maximum torque (ΔM) of rheometry were determined. Cure Rate Index is computed using the following equation:

$$\mathrm{CRI} = \frac{100}{T_{95} - T_{scorch}} \tag{1}$$

X-ray Diffraction. To study the degree of dispersion of the organoclay and increase in gallery spacing in the rubber composites, XRD studies were done using a PHILIPS X-PERT PRO diffractometer in the range of $2\theta = 1$–$10°$ and using Cu target ($\lambda = 0.154$ nm). In this experiment, acceleration voltages of 40 kV and beam current of 40 mA were used, and the scanning rate was maintained at 2°/min. The d-spacing of the organoclay particles were calculated using the Bragg's law ($\lambda = 2d\sin\theta$).

Field Emission Scanning Electron Microscopy. A field emission scanning electron microscope (FE-SEM; Hitachi microscope Model S-4160, voltage 20 kV, Japan) was used to study the morphology of the rubber nanocomposite fractured surfaces. Before the tests, the samples were fractured in liquid nitrogen. Afterward, the fracture surface was coated with gold and observed by FE-SEM.

Tensile Properties. The mechanical properties including the modulus 100%, tensile strength, and elongation at break of the NBR nanocomposites were investigated by the tensile test. Tensile properties were measured on dumbbell-shaped specimens punched out from the molded sheets. The tests were carried out as according to the ASTM D-412 method in a Universal Testing Machine (*Zwick-Roel*, model Z050, Germany). Tests were carried out at room temperature and cross-head speed of 500 mm/min. The result of tensile test for each sample was recorded as the average of three repeated observations.

Swelling Measurement. Swelling test in toluene solvent was conducted for the rubber compounds (25 mm × 15 mm × 2 mm) according to ASTM D 471-06. Initially, the dry weight of the samples was measured. Then, the samples were immersed in toluene at 25°C for 72 h; the swollen weight of the samples was recorded for the determination of the swelling ratio. The samples were periodically removed from the test bottles, the adhering solvent was cleaned from the surface, and the samples were immediately weighed. The swelling ratio can be calculated by the following equation:[55,56]

$$Q\ (\%\ \mathrm{mol}) = \frac{w_s - w_d}{w_d M_s} \tag{2}$$

where w_s and w_d are the weight of solvent adsorbed by the sample and the initial weight of sample, respectively. The volume fraction of rubber (v) and crosslink density (μ) can be determined from initial weight, swollen weight, and deswollen weight of the samples by using the well-known Flory–Rehner equation:[56]

$$v = \frac{1}{1 + \left\{\frac{w_s - w_{ex}}{w_{ex}}\right\}\left\{\frac{\rho_r}{\rho_s}\right\}} \tag{3}$$

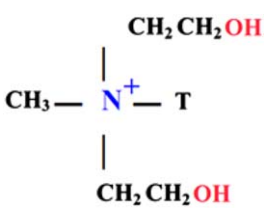

Figure 1. Modifier chemical structure for montmorillonite in Cloisite 30B, T is Tallow: carbon chains consist of 65% C18, 30% C16, and 5% C14. [Color figure can be viewed in the online issue, which is available at wileyonlinelibrary.com.]

Table II. Cure Rheometry Results for Pure NBR, SPFN, and DPFN Nanocomposites

CRI (min^{-1})	T_{95} (min)	T_s (min)	ΔM (dN m)	M_H (dN m)	M_L (dN m)	Vulcanizates
11.25	13.11	4.22	12.07	14.10	2.03	NBR
12.63	10.41	2.49	14.59	17.29	2.70	NC300
13.81	9.57	2.33	14.28	16.74	2.46	NC305
14.37	9.39	2.43	14.84	17.50	2.66	NC310
14.69	9.18	2.37	14.22	17.00	2.78	NC600
14.88	9.11	2.39	15.34	17.93	2.59	NC605
14.84	9.16	2.42	17.26	20.04	2.87	NC610

$$\mu = \frac{-[\ln(1-v)+v+\chi v^2]}{V\left[v^{\frac{1}{3}}-\frac{v}{2}\right]} \quad (4)$$

where w_{ex} is sample dried weight after swelling, ρ_r and ρ_s is the density of the rubber compound (1 g/cm^3 for NBR) and solvent (0.86 g/cm^3 for toluene), respectively. V is the molar volume of the solvent (106.3 cm^3/mol) and χ is the Flory–Huggins polymer–solvent interaction term ($\chi = \chi_0 + \beta v$, $\chi_0 = 0.3809$ and $\beta = 0.6707$ for NBR-toluene at 298 K[56]). The thermodynamical parameters such as Gibbs free energy (ΔG) can be determined from the Flory–Huggins equation:[56]

$$\Delta G = RT\left[\ln(1-v) + v + \chi v^2\right] \quad (5)$$

where R and T are the universal gas constant (8.314 J/mol K) and the absolute temperature (298 K), respectively.

Dynamic–Mechanical Thermal Analysis (DMTA). The storage and loss modulus and the mechanical loss factor (tan δ) as a function of temperature were assessed by DMTA using Perkin–Elmer DMTA (model diamond) U.S.A in tension mode on rectangular specimens. The samples were scanned as a function of temperature from −100°C to 100°C at heating rate of 5°C/min and constant frequency of 10 Hz.

RESULTS AND DISCUSSION

Cure Characteristics

The obtained results from cure rheometry test are shown in Table II. M_H is a measure of modulus and the hardness of rubber compound. Crosslink density and effective interactions between polymer chains and filler results in higher M_H.[57] The ΔM is a measure of chemical cross-links (without considering physical cross-links). Also M_L is related to physical crosslinks in gum or uncured state or chain entanglement with each other.[57] Also this parameter could be a good measurement of physical properties to consider the comparison of tensile and tear strength and other properties. ΔM depends on the amount of cross-links, filler content and filler dispersion in matrix and also interfacial interactions.[57]

Addition of organoclay to NBR increases M_L and M_H. An interesting point is that viscosity decreases in gum state with nano-$CaCO_3$. This can be due to spherical shape and also modified surface of nano-$CaCO_3$ by fatty acids that can cause easier movement of chains which results in decrease of viscosity and M_L. This trend for M_L is also reported in NR.[1]

In hybrid nanocomposites with increase of nano-$CaCO_3$, an increased trend for M_H and ΔM is seen. Similar phenomenon are also true for nanocomposites as with the increase of nano-$CaCO_3$ due to higher intercalation and surface area between nanofiller and chains this will cause increasing cure rheometry parameters. However, we should not ignore the reinforcing effect of nano-$CaCO_3$. Calcium carbonate nanoparticles cause reduction in M_L, but addition of this nanofiller to NBR-containing organoclay causes increase in M_L. Considering the cure rheometry results, it seems that optimum concentration of nano-$CaCO_3$ in hybrid systems is 10 phr because highest increase in M_H and ΔM is shown in NC610 nanocomposite. Substantially, dispersion of fillers specifically organoclay nanolayers have better condition in these nanocomposites therefore higher torque for flowing them is required.

Increase of ΔM in hybrid nanocomposites containing 6 phr organoclay is higher than single-filler phase nanocomposites (SFPNs) which is showing reinforcing effect of simultaneous usage of two nanoparticles. Rubber chains under high shear rate forces in the melt mixing process puts them between organoclay galleries. In consideration of nanolayers structure, mobility of trapped chains is much reduced and therefore this is the reason for increase in torque rheometry. Arroyo *et al.*[58] in compatibilized NR nanocomposites by using ENR showed that addition of different organoclays would not make any significant changes in M_L and Mooney viscosity. These kinds of changes in cure rheometry parameters shows reinforcement effect of organoclay with nano-$CaCO_3$ in NBR.

Effects of nano-$CaCO_3$ and organoclay on scorch and optimum cure time of NBR were studied and the results show that organoclay causes reduction in scorch time and optimum cure time, although its concentration has no significant change on these parameters. Also, using nano-$CaCO_3$ in the presence of organoclay does not show any significant change on time parameters of cure rheometry. The CRI is calculated using the eq. (1). Addition of organoclay caused CRI to increase. Use of nano-$CaCO_3$ has no significant change on this index. Based on some reports,[59,60] specifically in sulfur vulcanization of rubber nanocomposites, amine molecules existing in organoclay galleries are willing to co-operate in vulcanization reaction. Also it seems that nano-$CaCO_3$ has no significant effect on the curing process, specifically sulfur curing mechanism in NBR compounds.

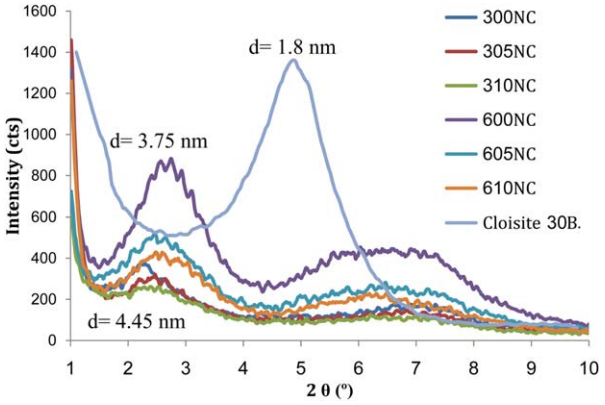

Figure 2. X-ray diffraction patterns for Cloisite 30B and NBR nanocomposites. [Color figure can be viewed in the online issue, which is available at wileyonlinelibrary.com.]

Morphological and X-ray Diffraction Studies

X-ray Diffraction. In order to study the microstructure and dispersion of organoclay in NBR, X-ray diffraction (XRD) analysis and scanning electron microscope were used. Organoclay's and NBR nanocomposite's XRD patterns are shown in Figure 2. The XRD pattern of organoclay revealed a characteristic diffraction peak at $2\theta = 2.8°$, corresponding to a basal spacing of 1.8 nm and also its peak has a high intensity. This space in nanocomposite containing 3 phr organoclay (NC300) increases by about 4.49 nm and peak location was transferred to lower angles due to intercalation of NBR. The nanocomposite containing 6 phr organoclay (NC600) have two peaks at $2\theta = 2.3°$ and 6.8°. Based on Bragg equation, the positions of these peaks are d-spacing = 4.4 nm and 1.5 nm. Bigger d-spacing indicates significant diffusion of rubber chains in silicate nanolayers. On this basis, d-spacing in contrast to original state has increased about 2.69 nm. With reference to the obtained XRD patterns, intercalated structure is expected for NBR nanocomposites (SFPNs and DFPNs).

The effects of adding 5 phr nano-$CaCO_3$ to NBR nanocomposites containing 3 phr and 6 phr show that peak intensity is reduced and d-spacing does not show any significant changes. With the addition of 10 phr nano-$CaCO_3$ (NC310), still the same situation is in place [Figure 3(A)]. Adding co-reinforcer (nano-$CaCO_3$ as second filler) to the system causes decrease agglomeration, which results in the break of filler agglomeration and better nanodispersion. The decrease of peak intensity by addition of co-reinforcer to SFPN leads to decrease tactoid size of organoclay. Better exfoliation of organoclay can be caused by nano-$CaCO_3$ incorporation and by collisions and friction between nano-$CaCO_3$ particles and organoclay platelets during mixing process of compound. The higher loadings of nano-$CaCO_3$ create more collisions with organoclay and therefore nano-$CaCO_3$ can support better exfoliation of the organoclay platelets. This phenomenon can be related to higher performance of hybrid nanocomposite other than SFPNs. Similar phenomenon is also observed for nanocomposites containing 6 phr organoclay. As organoclay concentration in nanocomposite increases, X-ray peak intensity increases too. The addition of nano-$CaCO_3$ also reduces peak intensity and increases d-spacing. For NC600 nanocomposite, d-spacing is about 3.75 nm which has increased for NC605 and NC610, respectively, to 3.93 nm and 4.20 nm.

In the next sections, improvements that are made in the properties of NBR nanocomposites are discussed. Reduction of peak intensity can also indicate reduction of size stacks or in another word reduction of number of layers in each stack. This is because of the increase in shear stress in mixing step for the preparation of nanocomposites that causes convenient peeling of organoclay layers. In other papers, also it has been reported that adding second filler has a positive effect on intercalation process and creates more idealistic morphology.[37, 43]

Considering patterns that are obtained, it should be noted that peak intensity of nanocomposites not reaches zero. Therefore, the probability of exfoliated structure formation in the NBR matrix is none. This kind of nanolayers catch bigger d-spacing due to extensive shear stress; however, they do not lose their primary arrangement.

According to XRD analyses, using two fillers simultaneously in polymer matrix creates nanocomposites with better morphology

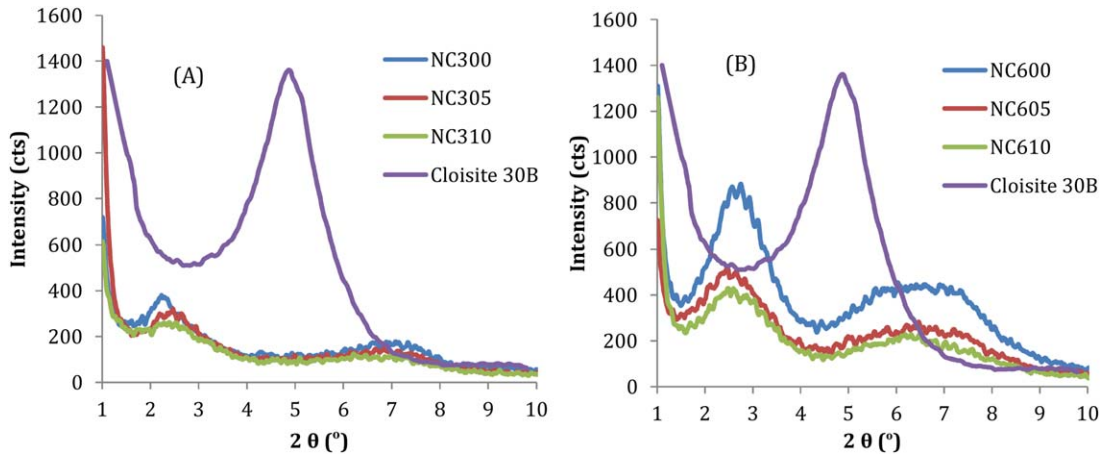

Figure 3. X-ray diffraction patterns of hybrid NBR nanocomposites: (A) containing 3 phr organoclay and (B) containing 6 phr organoclay. [Color figure can be viewed in the online issue, which is available at wileyonlinelibrary.com.]

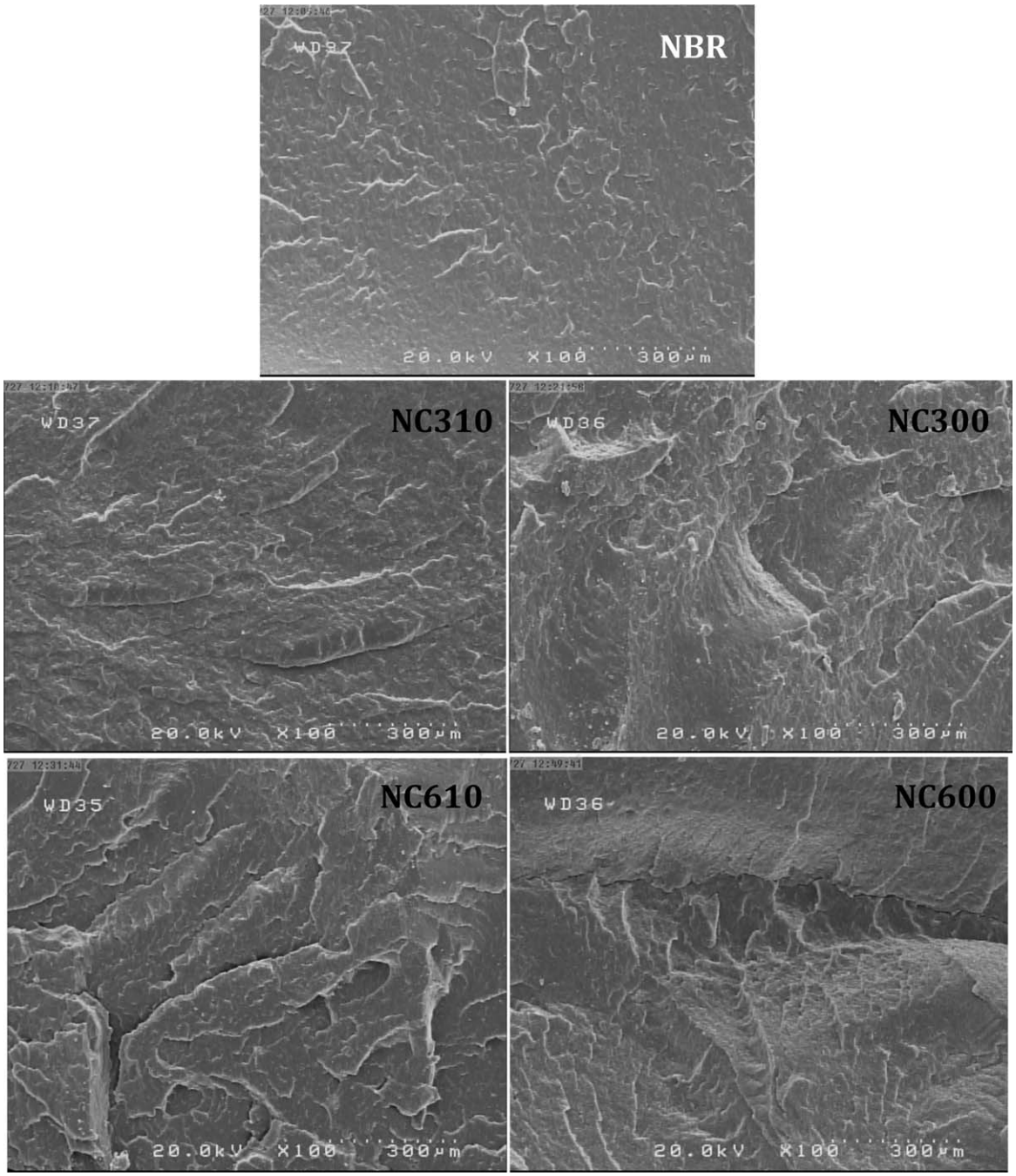

Figure 4. FE-SEM micrographs of NBR nanocomposites (magnification 100×).

than ordinary single-filler phase nanocomposites (SFPNs). Therefore, use of this idea is suggested in the preparation of high-quality nanocomposites, specifically in matrices with high molecular weight in which distribution is more difficult. Still final decision on this phenomenon requires much more study on morphology, physical and mechanical aspects. Next we will study more regarding this in this article.

Scanning Electron Microscopy. Investigation of filler dispersion in the NBR matrix and the effect of nanoparticles on the fracture morphology of prepared nanocomposite were studied by the FE-SEM. FE-SEM micrographs of pure NBR, SFPN, and DFPN nanocomposites in various magnifications are shown in Figures 4–6. In 100× magnification (Figure 4), the addition of nanoparticles and also increase in concentration causes increase in roughness fracture surface. This phenomenon is better seen in higher magnification, specifically 300× (Figure 5). A significant change in surface fracture morphology is created with the addition of nanofillers to NBR. Accordingly, the smoothness of fracture surface is removed. Higher roughness in fracture surface can be the reason of higher reinforcing effect of nanofillers and especially organoclay compared to the nano-$CaCO_3$.[61]

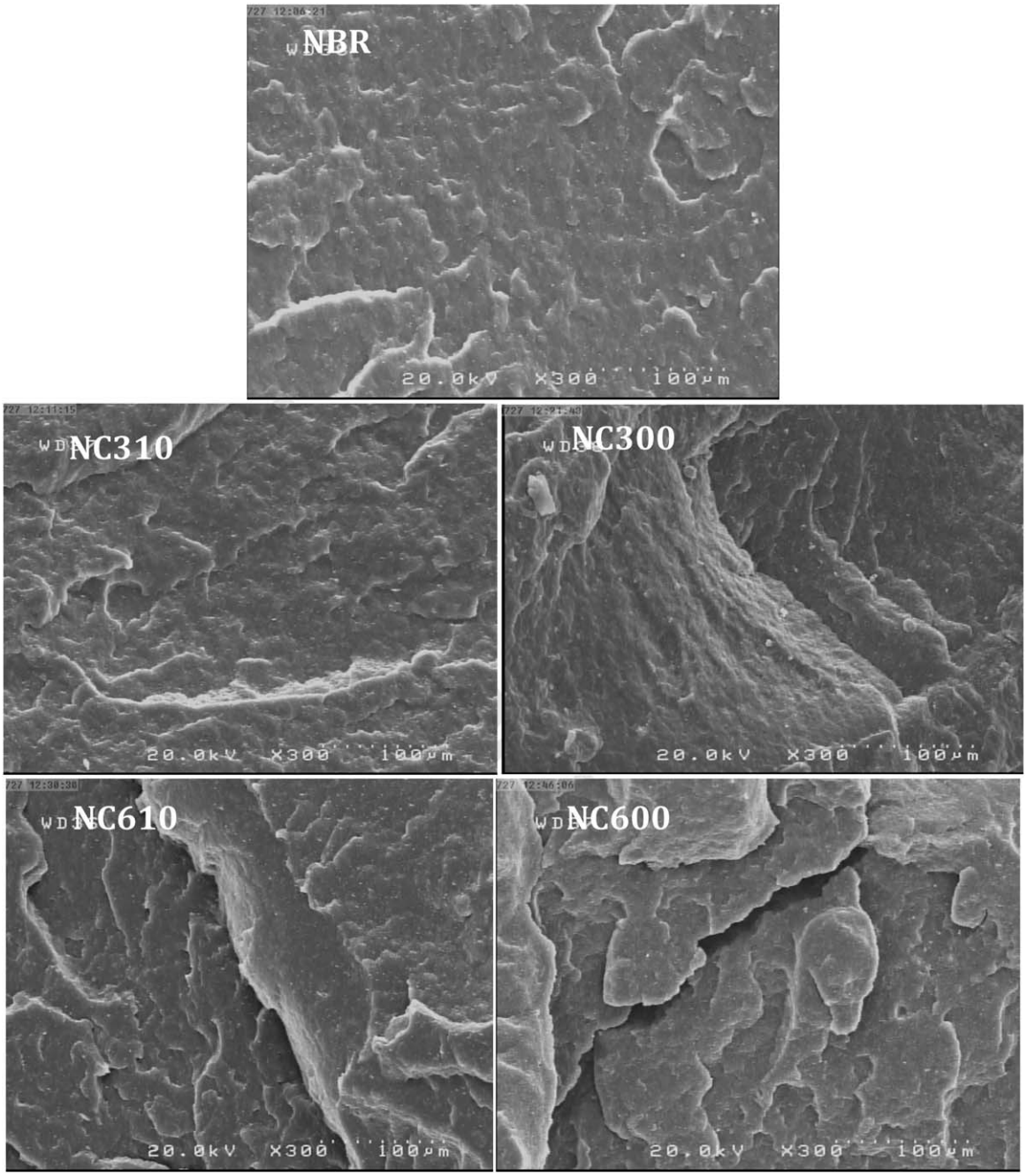

Figure 5. FE-SEM micrographs of NBR nanocomposites (magnification 300×).

In the very high magnifications (3000×, Figure 6), micrographs shows adequate dispersion of organoclay and nano-$CaCO_3$ in NBR matrix. The appropriate dispersion of organoclay and nano-$CaCO_3$ in the matrix was considered as the main reason for high mechanical efficiency of hybrid nanocomposites. So, it can be concluded that use of co-reinforcer leads to improve filler dispersion, particularly organoclay in rubber matrix.

An interesting point in micrographs is the existence of dark dots (small holes) in the single-phase filler nanocomposites (NC600 and NC300), which were eliminated by the addition of nano-$CaCO_3$ to these nanocomposites (NC610 and NC310) (Figure 6). These points come from the filler pull out from the matrix. Such cavities indicate weaker wetting and filler–matrix adhesion.[61,62]

Many agglomerations of nanoparticles are seen in NC300 nanocomposite. Adding nano-$CaCo_3$ to this nanocomposite (NC310) removes agglomeration. Increasing organoclay content has placed better dispersion and it is more in the presence of nano-$CaCO_3$ (NC610). According to the presented micrographs, none agglomeration of nano-$CaCO_3$ and organoclay is observed and in another word a much improved morphology is created for the hybrid nanocomposites. Such a phenomenon has been

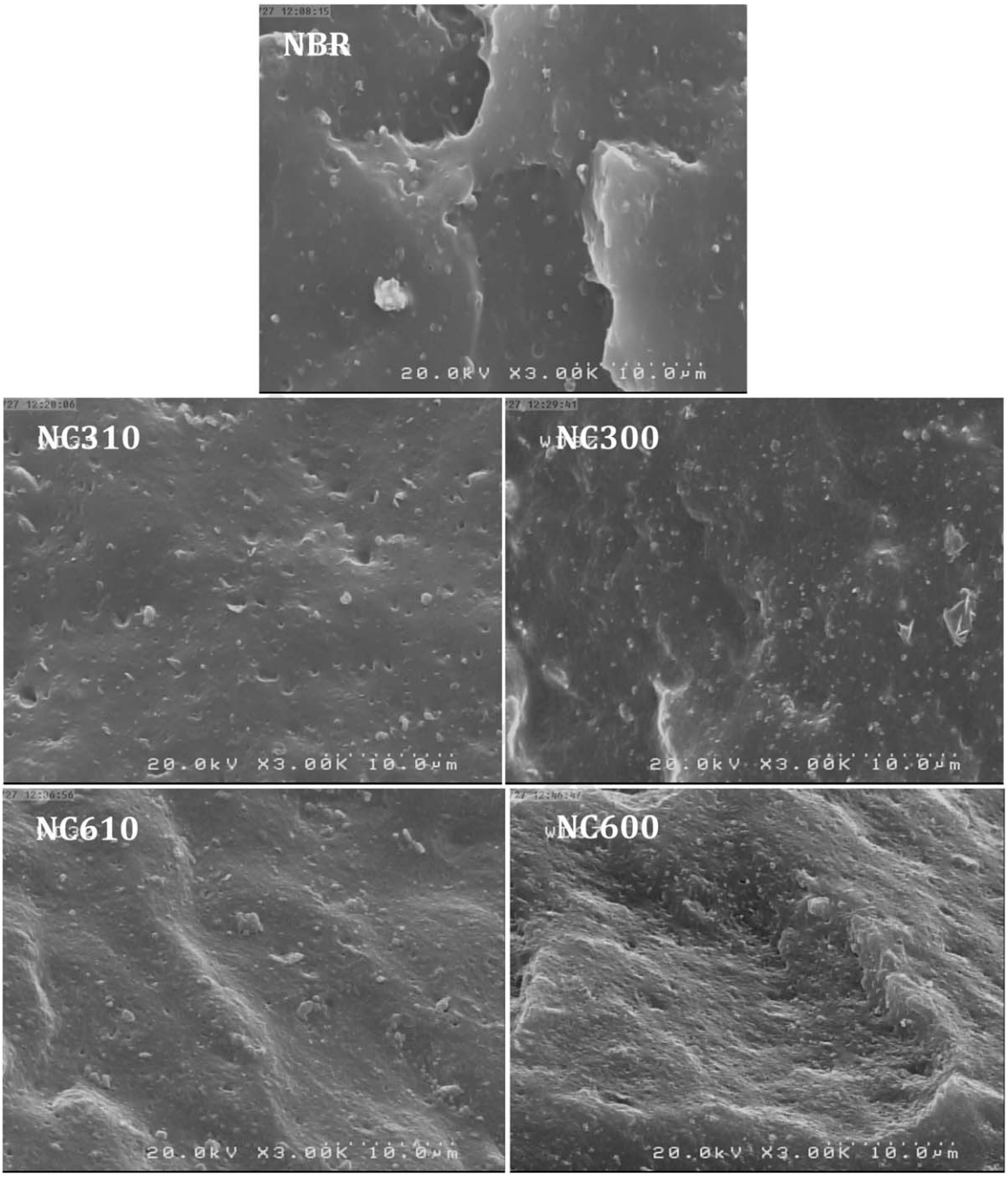

Figure 6. FE-SEM micrographs of NBR nanocomposites (magnification 3000×).

reported by Bokobza[5] for SBR nanocomposites reinforced by carbon nanotube and CB, Ratanasom[8] for NR/organoclay/CB nanocomposites, and Zare[63] for PP/organoclay/nano-$CaCO_3$ nanocomposites. Such a good dispersion of nanolayered silicate and nano-$CaCO_3$ in NBR is considered as the main factor for the substantial improvement of mechanical and swelling properties.

Tensile Properties of NBR Nanocomposites. Tensile test was used in order to study the mechanical behavior of NBR nanocomposites including single-filler phase nanocomposites and double-filler phase nanocomposites. To run this comparison, also a reinforced conventional NBR compound by 30 phr CB was tested. All the results are shown in Table III.

The addition of organoclay to NBR improved modulus, tensile strength, and elongation at break of these nanocomposites. According to that, addition of 3 phr and 6 phr organoclay increases the tensile strength of the NBR from 1.94 to 3.42 MPa and 4.88 Mpa, respectively. Using nano-$CaCO_3$ in hybrid nanocomposites also shows sensible increase in modulus, tensile strength, and elongation at break.

Table III. Tensile Test Results for Pure NBR and Its Nanocomposites

Vulcanizates	Modulus 100% (MPa)	Tensile strength (MPa)	Elongation at break (%)
NBR	1.12 ± 0.08	1.94 ± 0.19	320 ± 27
NC300	1.17 ± 0.08	3.42 ± 24	588 ± 31
NC305	1.18 ± 0.06	3.62 ± 0.21	637 ± 26
NC310	1.20 ± 0.05	4.25 ± 0.18	695 ± 15
NC600	1.42 ± 0.07	4.88 ± 0.19	668 ± 26
NC605	1.33 ± 0.04	5.47 ± 0.16	802 ± 21
NC610	1.48 ± 0.07	8.72 ± 0.26	1006 ± 37
NBR/CB-30	2.20 ± 0.16	10.69 ± 0.44	435 ± 19

According to the obtained results, 6 phr organoclay can increase the tensile strength to more than double of its original measure. Hybrid filler system causes increase in modulus, tensile strength, and elongation at break of NBR, and this shows that organoclay and nano-$CaCO_3$ have significant role in reinforcing NBR.

According to the other tests such as cure rheometry and swelling, NC610 nanocomposite has the optimum behavior. Tensile test is also miscible with cure rheometry, morphological studies, and swelling behavior. Addition of mentioned fillers to NBR creates the best chain intercalation level and also least amount of nanoparticles agglomeration in the system. Therefore, by using 6 phr organoclay and 10 phr nano-$CaCO_3$, strength of NBR can be improved about three times (350%). Elongation at break for these nanocomposites has an interesting pattern. Although elongation at break of NBR has been improved about 350% by incorporation of 6 phr organclay and 10 phr nano-CaCO3. These significant properties are advantages of hybrid filler systems comparing to single filler systems. The lower elasticity of conventional compound containing CB in comparison to hybrid nanocomposites is one of the major disadvantages of conventional fillers (such as CB) and also single-filler phase system that causes loss of rubber elasticity. In other words, improvement of mechanical properties gained without losing elasticity properties by the production of hybrid nanocomposites.

These phenomena are also reported for NR reinforced by organoclay and CB.[37] In this report, improvement of tensile strength in hybrid nanocomposites is 147% compared to pure NR; however, in our report, improvement of tensile strength in NBR reinforced by organoclay and nano-$CaCO_3$ is about 350%. Regarding the improvement of exfoliation process of organoclay (which was proved by XRD) and to minimize the mobility of the chains, it can be seen that nano-$CaCO_3$ can increase the elongation at break. This phenomenon can be related to spherical shape and also surface modification of nano-$CaCO_3$ by fatty acids, which cause slippage and higher mobility of chains.

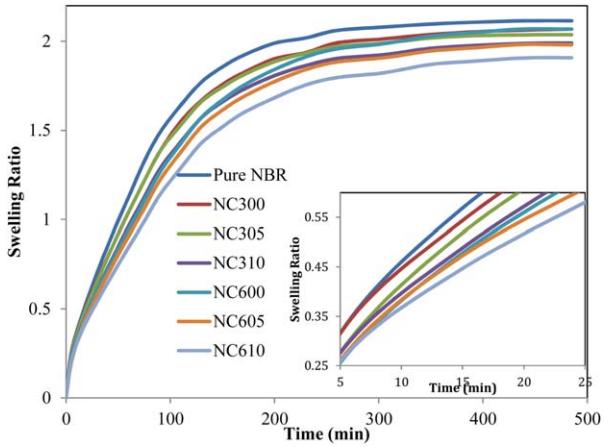

Figure 7. Swelling behavior of NBR and its nanocomposites in room temperature and toluene solvent. [Color figure can be viewed in the online issue, which is available at wileyonlinelibrary.com.]

Swelling Behavior. This is an appropriate measurement for swelling quality, cross-link density, mechanical properties, and evaluation of physical and chemical interactions between polymer matrix and nanofiller. Swelling behavior results for NBR and its nanocomposites are shown in Figure 7 and the measured parameters are presented in Table IV.

Swelling of vulcanizates in solvents proves to be an effective method to determine the chemical crosslink density.[64] The degree of adhesion between rubber chains and filler particles could be evaluated by the equilibrium swelling of the composites in good solvents. With increase the filler content, equilibrium swelling ratio of nanocomposites decreased and the rate of solvent uptake also decreased too (Table IV). The decrease of swelling coefficient by filler content has been attributed to the lesser mobility of the macromolecular chains. As could be observed, the apparent cross-link density of nanocomposites increased with increase the organoclay content. Increase in

Table IV. Swelling Parameters for NBR and Its Nanocomposites

ΔG(J/mol)	Apparent crosslink density ($\times 10^5$)	Interaction parameter (χ)	Volume fraction	Swelling ratio	Vulcanizates
−10.65	7.708	0.5837	0.302	2.11	NBR
−10.94	7.964	0.5877	0.308	2.01	NC300
−10.96	7.975	0.5885	0.309	1.88	NC305
−11.33	8.219	0.5931	0.316	1.76	NC310
−10.96	7.975	0.5883	0.309	1.94	NC600
−11.73	8.499	0.5941	0.319	1.78	NC605
−11.81	8.540	0.5982	0.324	1.64	NC610

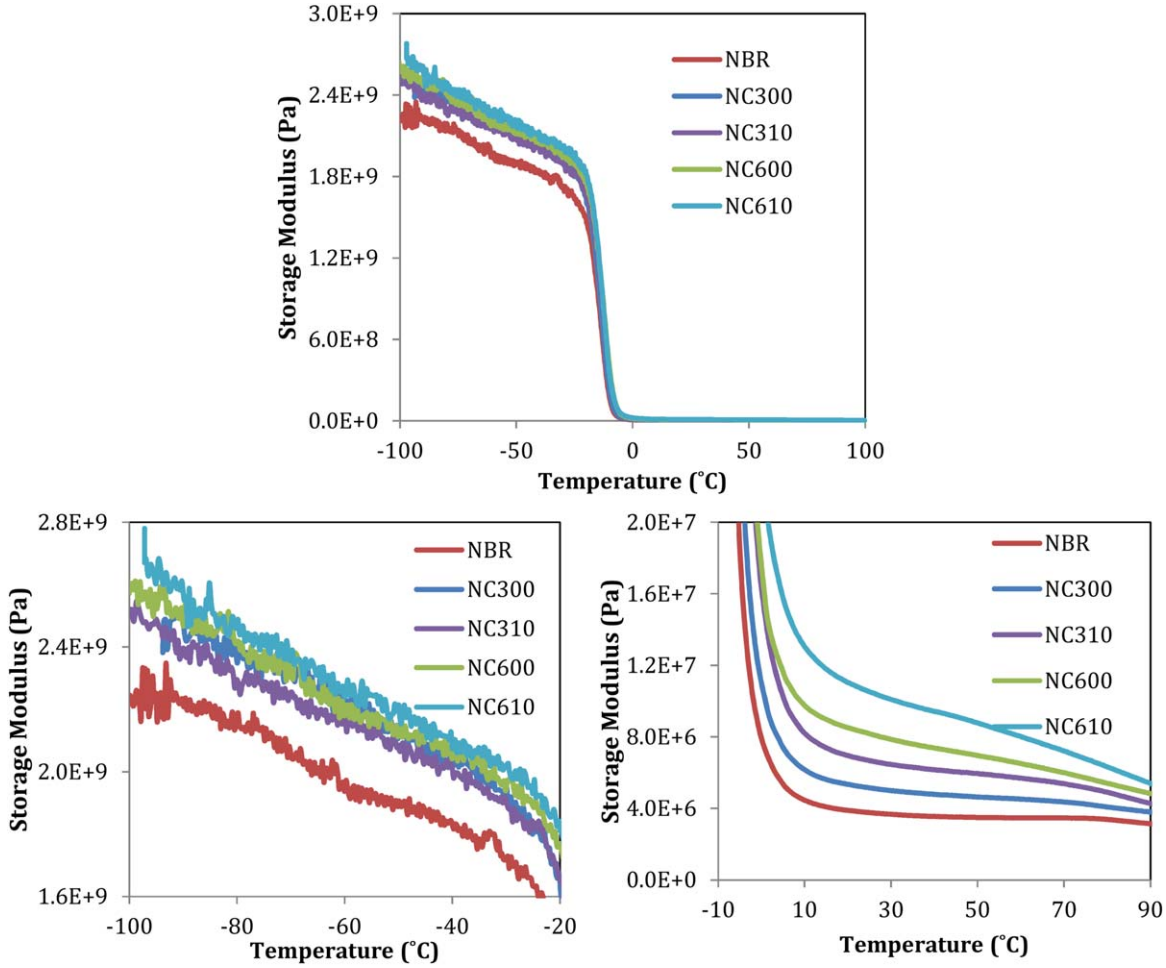

Figure 8. Changes in storage modulus for NBR and its nanocomposites in glassy and rubbery regions. [Color figure can be viewed in the online issue, which is available at wileyonlinelibrary.com.]

cross-link density was due to the activating effect of organoclay on cure process and also restriction of rubber chains in the presence of nanofiller. As the filler content increases, the rubber chains are maintained in a more restricted fashion, which resists the uptake of solvent.[65] Impermeable filler particles in the matrix cause the tortuous path to solvent diffusion and this could reduce the ultimate swelling of nanocomposites.[66] If filler is immiscible with the polymer, the interphase will consist of small cavities that can acts free volume in system. These cavities are readily available for the solvent molecules and hence the permeability of composite increase.

For these kinds of nanocomposites with the addition of organoclay, swelling ratio has reduced and caused volume fraction and cross-link density to increase. While in hybrid systems with the addition of nano-$CaCO_3$ and also increase its concentration, significant increase in volume fraction and cross-link density is shown. On this basis, once more advantages of hybrid systems compared to other nanocomposite systems are considered. Note that the obtained results from swelling test are actually very compatible to cure rheometry, morphological analysis, and also mechanical properties.

According to the obtained results in previous sections, existence of co-reinforcer filler next to each other filler can produce better dispersion for both nanofillers in rubber matrix. Also this phenomenon can be accounted for the higher surface area of nanofillers with NBR matrix in hybrid nanocomposites when compared to single-filler phase nanocomposites. As the surface area of nanofiller and interfacial interactions increases, most chains trapped in organoclay galleries and swelling ability will be lost. Improvement of swelling resistance especially in hybrid nanocomposites is because of the existence of hard filler phase and is impermeable to the solvent molecules.

The free energy values were observed to be negative in all cases, indicating spontaneity of the process and indicate that the sorption is favorable for all samples. ΔG is related to the elastic behavior of vulcanizates. Addition of organoclay to the NBR and its increase could result better elasticity for the nanocomposite and can be related to limited chains mobility in the presence of nanofiller.[67] Also miscibility between polymer and filler is expressed another reason to increase the Gibbs free energy.[68] The obtained results in agreement with Mousa *et al.*[69] in the thermodynamic analysis of SBR/Clay nanocomposites in

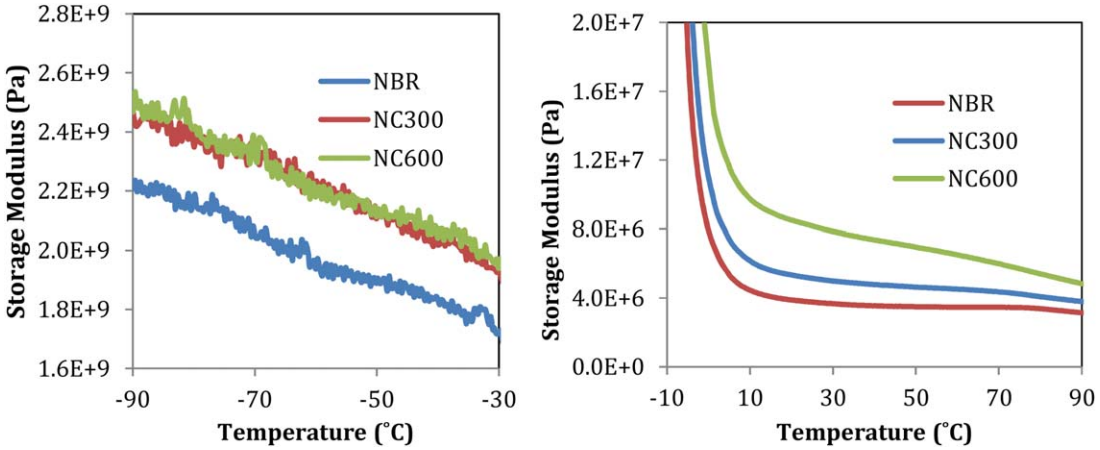

Figure 9. Effect of organoclay on storage modulus of NBR in glassy and rubbery regions. [Color figure can be viewed in the online issue, which is available at wileyonlinelibrary.com.]

chloroform solvent. It should be noted that ΔG increases in the presence of organoclay and nano-$CaCO_3$. It is assumed that ΔG is closely related to the elastic behavior of the material, i.e., the nanocomposites show a better elasticity than the pure NBR. These results can be attributed to the better dispersion of nano-silicate and nano-$CaCO_3$ in matrix. The better dispersion and higher interfacial interaction between filler and rubber is responsible for the increase of ΔG as compared with pure NBR.

Dynamic–Mechanical Thermal Analysis. Dynamical-mechanical analysis has been used to measure the viscoelastic properties of polymers and also evaluation of interaction between polymer and nanofiller.[70] Changes of storage modulus versus temperature for pure NBR and NC300 and NC600 nanocomposites and hybrid nanocomposites (NC310 and NC610) are shown in Figure 8.

In Figure 9, the effects of adding organoclay to NBR and increase concentration in single phase filler systems are provided. On this basis, with the addition of organoclay to NBR, storage modulus in rubbery region (higher than glass transition temperature) increases significantly. Increase in modulus is because of the reduction in chain mobility and activity. When rubber chains locate in galleries, they traps in this space, therefore volume fraction of filler in nanocomposite increases and this is the cause of higher storage modulus in nanocomposites with intercalated structure. As more degree of this structure creates in matrix, the storage modulus will be higher.

Effect of simultaneous addition of the two nanofillers and also changes in concentration of nanoparticles on storage modulus behavior is shown in Figure 10. As shown, nano-$CaCO_3$ in hybrid nanocomposites affect the storage modulus significantly. Hybrid nanocomposites in glassy region have higher storage modulus compared to single filler phase systems. This large increase in storage modulus has a more physical cause (filler–filler interaction) than chemical cause (filler–polymer interaction).[49]

Nano-$CaCO_3$ next to organoclay results in higher storage modulus in glassy, transition, and rubbery regions that this for another time proves the advantages of using these two nanocomposites on NBR. Also higher cross-link density in hybrid nanocomposites can also be another reason for higher storage modulus in all the regions. By measuring cross-link density for various nanocomposites, it has come to our attention that hybrid nanocomposites have higher crosslink density. Also this phenomenon can be linked to improved intercalation process (in comparison to single filler organoclay compounds) with the addition of nano-$CaCO_3$.

Damping Factor (tan δ). tan δ represents converted work to heat to retrieved work based on certain amount of work. It must be considered that the smaller peak of glass transition temperature represents higher reinforcing performance of filler. Figure 11 shows a comprehensive comparison of the variations in tan δ of NBR and single and hybrid filler based nanocomposites. The addition of organoclay causes NBR's glass transition temperature to small change. On this basis, glass transition temperature of pure NBR changes from -7°C to -6°C by 6 phr organoclay. Furthermore, it can be observed that organoclay reduced peak height (tan δ) and this also proves less energy dissipation by rubber chains in these types of nanocomposites. More interaction between polymer and filler improves the elasticity of nanocomposite which results in lower tan δ and transition of this peak to higher temperatures.[71] Reduction of tan δ can be related to strong interaction in polymer–filler interface. This reduction due to the addition of organoclay has been reported in other reports.[70, 71] Reduction in tan δ can be considered as a measurement for the formation of higher degree of intercalated structure. The addition of nano-$CaCO_3$ is to improve the chain intercalation process. As observed in the XRD analysis, nano-$CaCO_3$ increases chain intercalation which it can be also proved by dynamic–mechanical analysis.

CONCLUSIONS

Attempts have been made to prepare a new generation of rubber nanocomposite by using organoclay and nano-$CaCO_3$. To do this, several compounds based on NBR containing different content of organoclay and nano-$CaCO_3$ were prepared by using melt mixing process. However, there is no published information on the production of hybrid NBR nanocomposites including organoclay and nano-$CaCO_3$. In addition to mechanical testing, the dispersion state of the nanofillers into NBR was

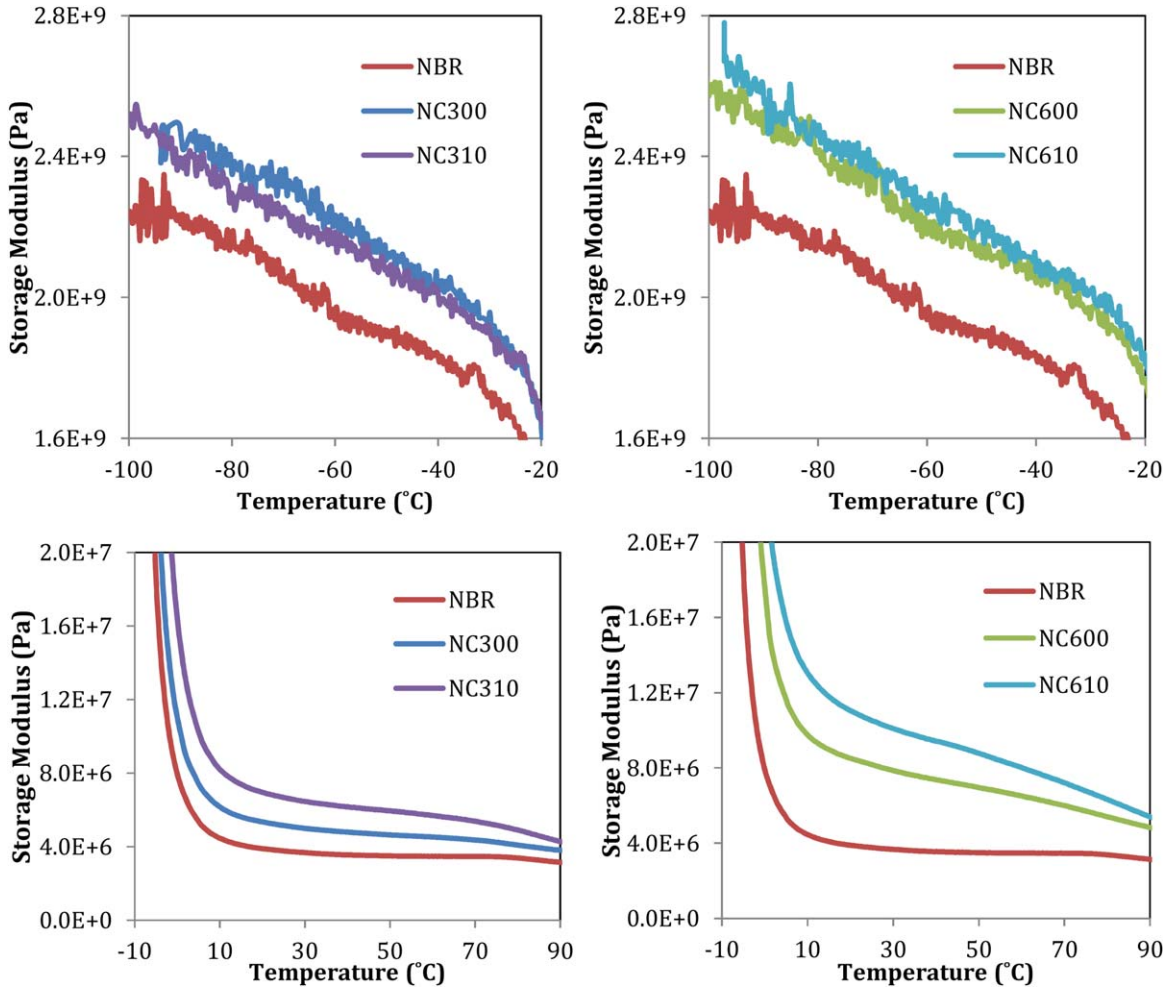

Figure 10. Changes in storage modulus in glassy and rubbery region for pure NBR, single and dual phase fillers nanocomposites. [Color figure can be viewed in the online issue, which is available at wileyonlinelibrary.com.]

studied by XRD, FE-SEM as well as DMTA in order to understand the morphology of the resulting nanocomposites. Morphological studies showed that the collisions and friction between nano-$CaCO_3$ particles and organoclay could support intercalation and exfoliation of organoclay during mixing process. Synchronous use of nanofillers to NBR leads to better dispersion of nanofillers because the collisions and friction of nanoparticles and nanolayers, so leading to breakdown of filler agglomerates. Based on the morphological analysis, a very proper relationship between structure and properties of NBR/organoclay/nano-$CaCO_3$ hybrid nanocomposites is observed. The related results show that the optimized filler content in dual-filler phase nanocomposites (DFPNs) equals to 10 phr nano-$CaCO_3$ and 6 phr organoclay. The 350% improvement of tensile properties in nanocomposites reinforced with organoclay and nano-$CaCO_3$ revealed the synergistic effect of hybrid fillers systems against single-filler ones. So we can conclude that second filler (co-reinforcement) should be used to improve filler dispersion, particularly organoclay in rubber nanocomposites. It was observed that manufacture of nanocomposites with this approach showed better morphology, cure rheometry, swelling resistance, and mechanical properties compared with existing rubber products reinforced with single-phase filler, thus this approach has been introduced as an effective way to produce rubber nanocomposites.

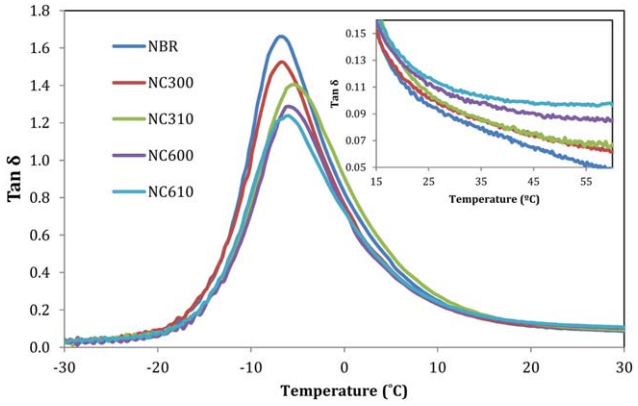

Figure 11. The effect of organoclay and nano-$CaCO_3$ on damping factor (tan δ) of NBR. [Color figure can be viewed in the online issue, which is available at wileyonlinelibrary.com.]

ACKNOWLEDGMENTS

The authors gratefully acknowledge the financial support provided by Young Researchers and Elite Club (Islamic Azad University-Omidieh Branch) for carrying out this study.

REFERENCES

1. Sobhy, M. S.; El-Nashar, D. E.; Maziad, N. A. *Egypt. J. Sol.* **2003**, *26*, 241.
2. Liu, L.; Jia, D.; Luo, Y.; Li, B. *Polym. Compos.* **2009**, *30*, 107.
3. Wang, S.; Zhang, Y.; Peng, Z.; Zhang, Y. *J. Appl. Polym. Sci.* **2006**, *99*, 905.
4. Rajasekar, R.; Pal, K.; Heinrich, G.; Das, A.; Das, C. K. *Mater. Des.* **2009**, *30*, 3839.
5. Bokobza, L.; Rahmani, M.; Belin, C.; Bruneel, J. L.; Bounia, N. E. *J. Appl. Polym. Sci.* **2008**, *46*, 1939.
6. Zheng, H.; Zhang, Y.; Peng, Z.; Zhang, Y. *J. Appl. Polym. Sci.* **2004**, *92*, 638.
7. Chattopadhyay, P. K.; Basuli, U.; Chattopadhyay, S. *Polym. Compos. 31*, 835.
8. Rattanasom, N.; Prasertsri, S. *Polym. Test.* **2009**, *28*, 270.
9. Maiti, M.; Sadhu, S.; Bhowmick, A. K. *J. Appl. Polym. Sci.* **2005**, *96*, 443.
10. Ahmed, Kh.; Nasir, M.; Imran, A.; Mahmood, Kh. *J. Mater. Environ. Sci.* **2014**, *5*(4), 1085.
11. Mousa, A.; Heinrich, G.; Gohs, U.; Wagenknecht, U. *J. Compos. Mater.* **2011**, *46*(10), 1151.
12. Ahmed, Kh. *J. Adv. Res.* **2015**, *6*, 225. DOI: 10.1016/j.jare.2013.12.002.
13. Mousa, A.; Heinrich, G.; Simon, F.; Wagenknecht, U.; Stöckelhuber, K. W.; Dweiri, R. *Mater. Res.* **2012**, *15*(4), 671.
14. Nigam, V.; Setua, D. K.; Mathur, G. N. *J. Mater. Sci.* **2001**, *36*, 43.
15. Lo, H. H.; Chu, C. F. China Steel Technical Report No. 24, **2011**, 40.
16. Ismail, H.; Haw, F. S. *J. Reinf. Plast. Compos.* **2010**, *29*, 105. DOI: 10.1177/0731684408096423.
17. Rattanasom, N; Saowapark, T; Deeprasertkul, C. *Polym. Test.* **2007**, *26*, 369.
18. Xiong, X.; Wang, J.; Jia, H.; Ding, L.; Dai, X.; Fei, X. *Polym. Compos.* **2014**, *35*, 1466.
19. Norimanand, N. Z.; Ismail, H. *Int. J. Polym. Mater. Polym. Biomater.* **2013**, *62*(5), 252.
20. Davoodi, A. A.; Khalkhali, T.; Salehi, M. M.; Sarioletlagh Fard, S. *J. Soft Matter* **2014**, Article ID 498563. *2014*, 1.
21. Kook, J. H.; Huh, M. Y.; Yang, H.; Shin, D. H.; Park, D. H.; Nah, C. *Polymer (Korea)* **2007**, *31*, 422.
22. Chen, S.; Yu, H.; Ren, W.; Zhang, Y. *Thermochim. Acta* **2009**, *491*, 103.
23. Zhan, Y. H.; Liu, G. Q.; Xia, H. S.; Yan, N. *Plast. Rubber Compos.* **2011**, *40*(1), 32.
24. Bokobza, L.; Rahmani, M.; Belin, C.; Bruneel, J. L.; Bounia, N. E. *J. Appl. Polym. Sci.* **2008**, *46*, 1939.
25. Cataldo, F.; Ursini, U.; Angelini, G. *Fullerenes Nanotubes Carbon Nanostruct.* **2009**, *17*, 38.
26. Thaptong, P.; Sirisinha, C.; Thepsuwan, U.; Sae-Oui, P. *Polym. Plast. Technol. Eng.* **2014**, *53*, 818.
27. Galimberti, M.; Coombs, M.; Riccio, P.; Ricco, T.; Passera, S.; Pandini, S.; Conzatti, L.; Ravasio, A.; Tritto, I. *Macromol. Mater. Eng.* **2013**, *298*, 241.
28. Ismail, H.; Ramly, A. F.; Othman, N. *Polym. Plast. Technol. Eng.* **2011**, *50*, 660.
29. Zavorka, Z. Properties and behaviors of polymeric systems containing mineral fillers, PhD thesis, Tomas Bata University, 2013.
30. Balachandran, M.; Devanathan, S.; Muraleekrishnan, R.; Bhagawan, S. S. *Mater. Des.* **2012**, *35*, 854.
31. Tarawneh, M. A.; Ahmad, S.; Zarina, K. K.; Hassan, I. N.; LihJiun, Y.; Flaifel, M. H.; ShamsulBahri, R. *Sains Malaysiana* **2013**, *42*(4), 503.
32. Zhang, H.; Wang, C.; Zhang, Y. *J. Appl. Polym. Sci.* **2015**, *132*, 41309.
33. Sadeghi Ghari, H.; Shakouri, Z. *Rubber Chem. Technol.* **2012**, *85*(1), 132.
34. Tzounis, L.; Debnath, S.; Rooj, S.; Fischer, D.; Mader, E.; Das, A.; Stamm, M.; Heinrich, G. *Mater. Des.* **2014**, *58*, 1.
35. Herrmann, W.; Uhl, C.; Heinrich, G.; Jehnichen, D. *Polym. Bull.* **2006**, *57*, 395.
36. Arroyo, M.; Manchado, M. A. L.; Herrero, B. *Polymer* **2003**, *44*, 2447.
37. Qu, L.; Huang, G.; Zhang, P.; Nie, Y.; Weng, G.; Wu, J. *Polym. Int.* **2010**, *59*, 1397.
38. Liu, Y.; Li, L.; Wang, Q. *J. Appl. Polym. Sci.* **2010**, *118*, 1111.
39. Sapkota, J.; Poikelispa, M.; Das, A.; Dierkes, W.; Vuorinen, J. *Polym. Eng. Sci.* **2013**, *53*,615.
40. Chattopadhyay, P. K.; Das, N. C.; Chattopadhyay, S. *Composites Part A* **2011**, 1049.
41. Chattopadhyay, P. K.; Basuli, U.; Chattopadhyay, S. *Polym. Compos.* **2010**, *31*, 835.
42. Gopi, J. A.; Patel, S. K.; Chandra, A. K.; Tripathy, D. K. *J. Polym. Res.* **2011**, *18*, 1625.
43. Wu, Y. P.; Zhao, W.; Zhang, L. Q. *Macromol. Mater. Eng.* **2006**, *291*, 944.
44. Praveen, S.; Chattopadhyay, P. K.; Albert, P.; Dalvi, V. G.; Chakraborty, B. C.; Chattopadhyay, S. *Composites Part A* **2009**, *40*, 309.
45. Ahmadi, M.; Abbasi, F.; Gharebaghi Tazehkand, H. *Iran. J. Sci. Technol. Polym.* **2008**, *21*(4), 339.
46. Galimberti, M.; Coombs, M.; Cipolletti, V.; Riccio, P.; Ricc, T.; Pandini, S.; Conzatti, L. *Appl. Clay Sci.* **2012**, 65, 57.
47. Malas, A.; Das, C. K. *J. Mater. Sci.* **2012**, *47*, 2016–2024, 2012.
48. Sridhar, V.; Shanmugharaj, A. M.; Kim, J. K.; Tripathy, D. K. *Polym. Compos.* **2009**, *30*, 6, 691.
49. Praveen, S.; Chattopadhyay, P. K.; Jayendran, S.; Chakraborty, B. C.; Chattopadhyay, S. *Polym. Compos.* **2010**, *31*, 97.

50. Bhattacharya, M.; Bhowmick, A. K. *J. Mater. Sci.* **2010**, *45*, 6126.
51. Jinnai, H.; Shinbori, Y.; Kitaoka, T.; Akutagawa, K.; Mashita, N.; Nishi, T. *Macromolecules* **2007**, *40*, 6758.
52. Liu, Y.; Li, L.; Wang, Q.; Zhang, X. *J. Polym. Res.* **2011**, *18*, 859.
53. Bhattacharya, M.; Bhowmick, A. K. *J. Mater. Sci.* **2010**, *45*, 6139.
54. Sadeghi Ghari, H.; Jalali Arani, A.; Shakouri, Z. *Rubber Chem. Technol.* **2013**, *86*(2), 330.
55. Shah, J.; Yuan, Q.; Misra, R. D. K. *Mater. Sci. Eng. A* **2009**, *523*, 199.
56. Zaborski, M.; Kunert, A.; Pietrasik, J.; Szynkowska, M. I.; Lesniewska, E. *Rubber Chem. Technol.* **2007**, *80*, 279.
57. Paul, K. T.; Pabi, S. K.; Chakraborty, K. K.; Nando, G. B. *Polym. Compos.* **2009**, *30*, 1647.
58. Arroyo, M.; Manchado, M. A. L.; Valentn, J. L.; Carretero, J. *Compos. Sci. Technol.* **2007**, *67*, 1330.
59. Varghese, S.; Kocsis, J. K. *J. Appl. Polym. Sci.* **2004**, *91*, 813.
60. Madhusoodanan, K. N.; Varghese, S. *J. Appl. Polym. Sci.* **2006**, *102*, 2537.
61. Jia, Q. X.; Wu, Y. P.; Wang, Y. Q.; Lu, M.; Zhang, L. Q. *Compos. Sci. Technol.* **2008**, *68*, 1050.
62. Li, Q.; Siddaramaiah, M.; Kim, N. H.; Yoo, G. H.; Lee, J. H. *Composites Part B* **2009**, *40*, 218.
63. Zare, Y.; Garmabi, H.; Sharif, F. *J. Appl. Polym. Sci.* **2011**, *122*, 3188.
64. Aprem, A. S.; Joseph, K.; Thomas, S. *Rubber Chem. Technol.* **2005**, *78*, 458.
65. Bhattacharya, M.; Maiti, M.; Bhowmick, A. K. *Rubber Chem. Technol.* **2008**, *81*, 782.
66. Meneghetti, P.; Shaikh, S.; Qutubuddin, S.; Nazarenko, S. *Rubber Chem. Technol.* **2008**, *81*, 821.
67. Li, P.; Wang, L.; Song, G.; Yin, L.; Qi, F.; Sun, L. *J. Appl. Polym. Sci.* **2008**, *109*, 3831.
68. Pojanavaraphan, T.; Schiraldi, D. A.; Magaraphan, R. *Appl. Clay Sci.* **2010**, *50*(2), 271.
69. Mousa, A.; Kocsis, J. K. *J. Macromol. Mater. Eng.* **2001**, *286*, 260.
70. Ahankari, S. S.; Kar, K. K. *Mater. Sci. Eng. A* **2008**, *491*, 454.
71. Pasquinia, D.; Teixeirab, E. M.; Curvelob, A. A. S.; Belgacemc, M. N.; Dufresne, A. *Industr. Crops Products* **2010**, *32*(3), 486.